



Research Article

Cell Detection Methods to Enhance the Sorting Rate of a Large-Cell Sorter

Shinnosuke Dowaki¹, Meito Fukada², Taiji Okano², Yosuke Tanaka^{1*}

¹Graduate School of Engineering, Department of Biomedical Engineering, Tokyo University of Agriculture and Technology, 2-24-16 Naka-cho, Koganei-shi, Tokyo 184-8588, Japan

²Graduate School of Bio-Applications and Systems Engineering, Tokyo University of Agriculture and Technology, 2-24-16 Naka-cho, Koganei-shi, Tokyo 184-8588, Japan

*Corresponding author: tyosuke@cc.tuat.ac.jp; Tel.: +81423887405; Fax: +81423887405

Abstract: Shrimp farming is widespread in Indonesia, and the risk of mass mortality due to disease outbreaks remains a significant concern. Recent research aimed at developing disease-resistant shrimp through genome editing has made remarkable progress. Additionally, the need for techniques that can efficiently isolate gene-edited cells is increasing. Currently, conventional cell sorters cannot be applied to millimeter-scale cells, such as egg cells; as a result, most isolation operations are still manual. To address this issue, we developed a millifluidics-based sorting system that selectively isolates only the fluorescently stained target cells from a population of large-sized cells. The sorting employs computer-based image processing, achieving high-purity sorting at a rate of 1.6 cells/s. This study aimed to improve the sorting rate while maintaining high purity by integrating the existing cell detection method with analog electronic fluorescence detection. As a result, a sorting rate of 2.85 cells/s was achieved even under non-optimized conditions, representing ~ 1.8 -fold increase in the sorting rate compared with that in a previous study. Because the cell detection speed is expected to be >10 times faster than previously described methods under optimized conditions, a sorting rate of >10 cells/s can be achieved in the future by further improving the detection circuit. This result represents a crucial step toward the practical implementation of high-speed and precision sorting technology for large cells.

Keywords: Analog electronic circuit; Cell sorter; Fluorescence detection; Large-cell sorting; Real-time signal detection

1. Introduction

In recent years, a rapidly growing demand has been observed for technologies that can efficiently isolate millimeter-scale spherical objects. Examples include fish eggs, cell aggregates (spheroids), and organoids, which have been appropriately isolated based on their morphological characteristics, fluorescent markers, or functional properties (Napitupulu et al., 2025; Azwani et al., 2025; Park et al., 2025; Pragiwaksana et al., 2024; Yousafzai and Hammer, 2023; Lu et al., 2023; Shen et al., 2021; Nie et al., 2021; Nurhayati et al., 2021; Sibuea et al., 2020; Sivaramakrishnan et al., 2020; Han et al., 2020; He et al., 2020; Liao et al., 2020). Such isolation is critical to various applications, including developmental biology, regenerative medicine, and drug screening (Liu et al., 2025; Nguyen et al., 2024; Lyu et al., 2020). The evaluation of genetic modifications and drug responses requires the efficient selection and isolation of target samples from large populations (Raffaele et al., 2025; Li et al., 2024; Chen et al., 2024; Cotta et al., 2024; Vo et al., 2024; Nitta et al., 2020; Isozaki et al., 2020).

However, high-speed and precision isolation technologies for large-sized cells are still being developed. In practice, genome-edited cell selection and isolation are still largely manual, with many inefficient steps that rely on the experience and visual-based judgment of the researcher.

Several automated isolation systems that utilize image processing have also been introduced, but the sequence of steps—imaging, image processing, target identification, and isolation—inevitably introduces temporal delays (Williams et al., 2025; Gao et al., 2025; Dinca et al., 2025; Zhang et al., 2024; Hanninen, 2024; Qiang et al., 2024; Jones et al., 2023; Capek et al., 2023; Naderi et al., 2021; Saito et al., 2021). A microfluidic-based sorting system for millimeter-scale cells has been recently reported. This method employs deep learning to determine whether each cell is a target or not, achieving a detection speed of ~ 10.6 ms/cell. However, the sorting process relies on robotic pipette manipulation, requiring ~ 3 s/cell (Diouf et al., 2024).

We previously developed a microfluidic-based sorter for large cells that captures cell images with a camera and determines if they are fluorescently stained through computer-based image processing (Fukada et al., 2021). In this system, sorting is achieved by switching the flow path immediately after detecting a target cell, thereby significantly increasing the sorting rate compared with manual or automated pipette-based isolation methods, with a maximum sorting rate of ~ 1.6 cells/s. Although our approach improved the sorting rate compared with the previous one, it remains insufficient for applications requiring high-speed and/or real-time processing. Furthermore, accelerating image processing requires GPUs with high processing performance and complex algorithms, thereby increasing the overall cost and power consumption. This study aimed to address these challenges by introducing an optical detection technique that does not rely on image processing and by developing a novel, efficient, and rapid sorting system applicable to millimeter-sized spherical objects. Specifically, we employed a method in which changes in light transmission, are instantly identified by an analog circuit as a fluorescently stained or unstained cell passes through the detection area of a millifluidic channel, enabling real-time signal processing and sorting decisions. This approach helps avoid the delays associated with image processing while achieving high-speed large-cell sorting at low cost and with low power consumption. The proposed method achieved a sorting performance that markedly exceeded the previous rate of ~ 1.6 cells/s, and it holds promise for the high-throughput processing of genome-edited large cells and spheroids. Additionally, it is expected to serve as a simple bio-experimental tool for educational settings and resource-limited environments. In this study, we focus on the development and performance evaluation of a real-time cell detection system based on an analog electronic circuit to verify its accuracy in detecting fluorescently stained millimeter-scale cells.

2. Materials and Methods

2.1 Sorting System

The previously developed large-cell sorting system consists of a millifluidic device with four channels: cell flow, cross-flow, sorting, and discard; a custom-designed cell dispenser connected to a syringe pump (YPS-202; YMC Co., Ltd., Kyoto, Japan), which introduces cells into the main flow path (cell flow channel) at regular intervals; a compressor-pressurized reservoir; a solenoid valve (VDW22JA; SMC Corporation, Tokyo, Japan); and an optical system connected to a computer for cell detection (Figure 1). This system identified the fluorescently stained target cells via image processing just before they reached the millifluidic device junction. The computer opened the solenoid valve when a target cell reached the junction, momentarily pressurizing the cross-flow channel to divert the stained cell into the sorting channel (Figure 2a). In contrast, unstained cells passed through the junction and were discarded (Figure 2b). Cells were introduced into the system using a syringe pump, and the sorting process was visually monitored using a microscope (LW-820T; WRAYMER Inc., Osaka, Japan).

This study adopted a method that instantly detects optical signals by employing an analog electronic circuit, without relying on a camera or image processing, to reduce delays in fluorescence detection and improve the sorting rate. Cells were introduced into the system using the same method as in our previously designed setup. Cell fluorescence was detected by a photo-sensor; the resulting changes in current triggered the solenoid valve, opening it instantaneously

(Figure 2c). This approach is expected to significantly shorten the overall processing time from cell detection to sorting, thereby enhancing the sorting rate.

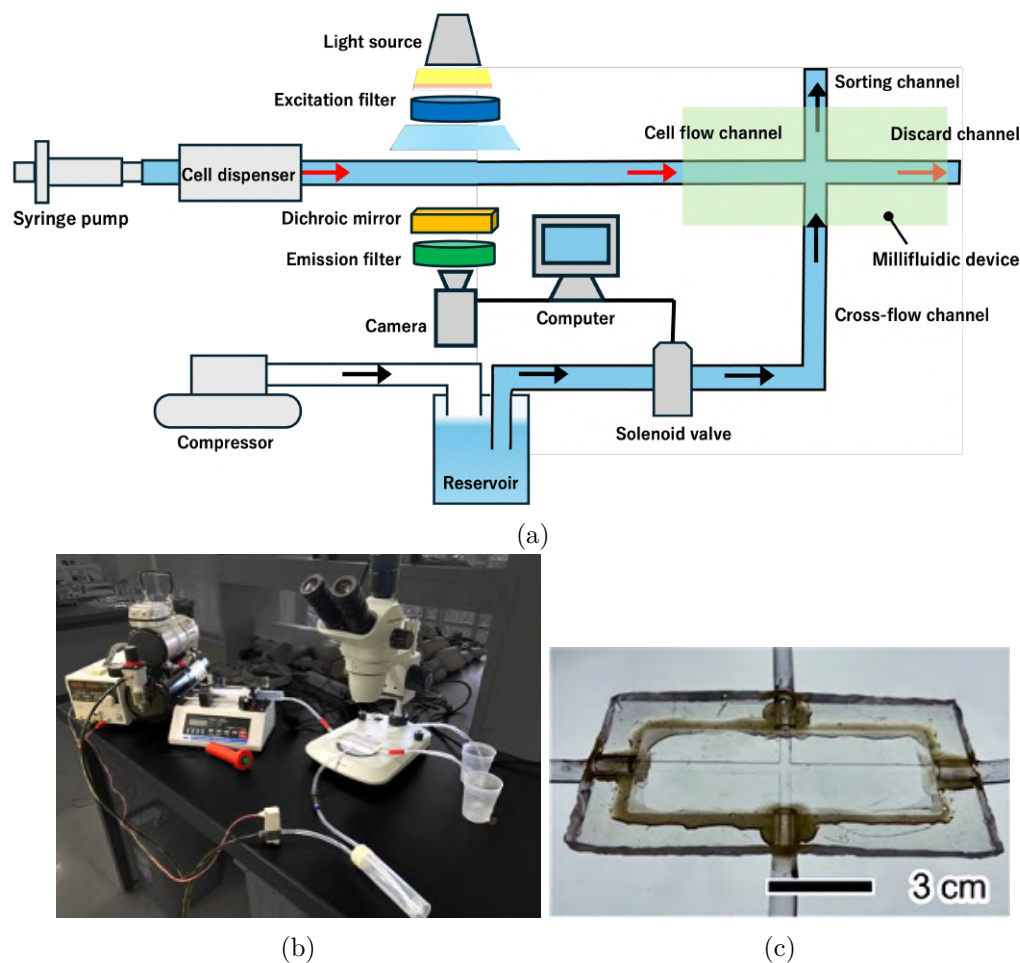


Figure 1 (a) Schematic and (b) photograph of the image processing-based large-cell sorting system developed in our previous study (c) Photograph of the millifluidic device

2.2 Cell preparation

In the experiment, we used easily obtainable flying fish eggs (diameter: 1.5–2.0 mm) as millimeter-scale spherical objects. Eggs were immersed in a 25 μM calcein solution (excitation: 495 nm; emission: 515 nm) for over 24 h to produce fluorescently stained cells (Figure 3).

2.3 The millifluidic device

The millifluidic device was fabricated using soft lithography techniques. The mold was designed with the 3D modeling software Blender and fabricated with an SLA-type 3D printer (Form 3; Formlabs, MA, USA) (Figure 4a). A mixture of a polydimethylsiloxane prepolymer (KE-106; Shin-Etsu Chemical, Tokyo, Japan) and curing agent (CAT-RG; Shin-Etsu Chemical) at 10:1 (w/w) was poured into the mold and cured on a hot plate at 60°C for 3 h. The PDMS was cut and demolded after curing. Subsequently, the PDMS and glass substrate were exposed to deep UV light (172 nm) for 3 min for surface activation. Then, they were bonded to each other by heating at 60°C for 30 min. Finally, the tubing and flow channel were attached with adhesive to complete the millifluidic device (Figure 4b). The dimensions of the channel through which cells pass are 6 mm in height, 4 mm in width, and 10 cm in straight length.

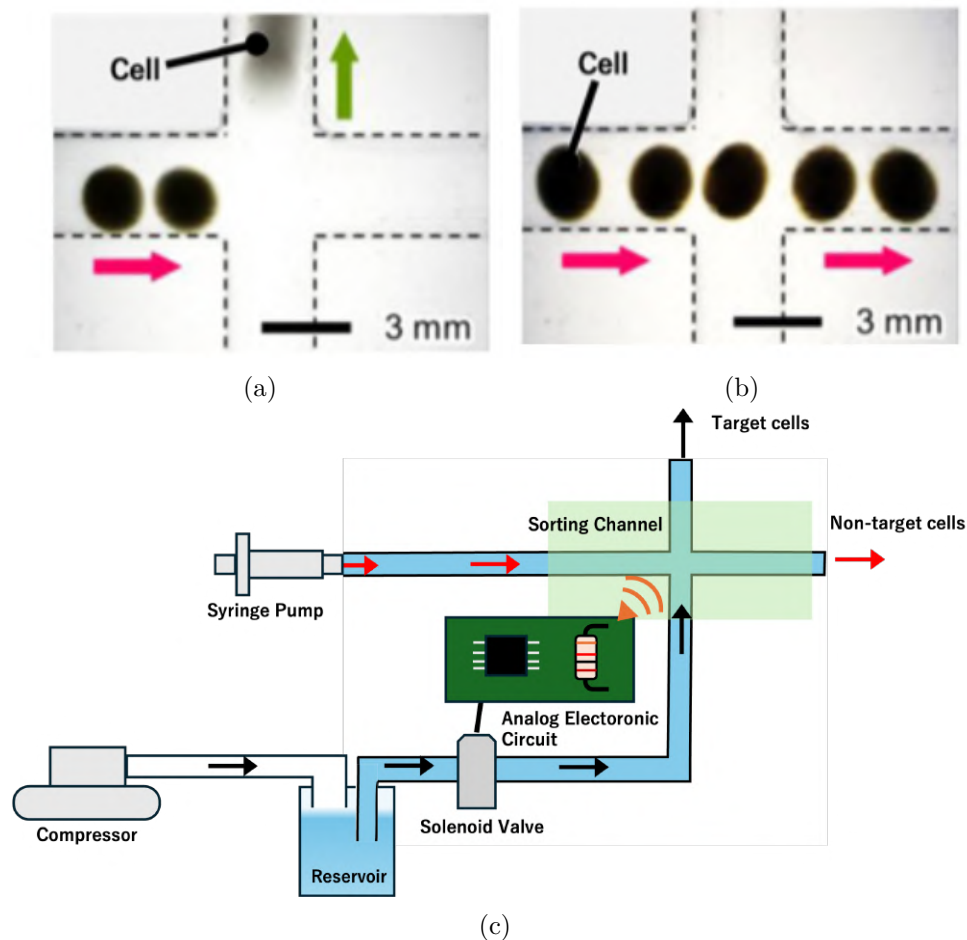


Figure 2 Images of (a) a target and (b) a non-target cell flowing near the millifluidic device junction. Each image is a composite of snapshots captured at 25 ms intervals. The dashed lines indicate the channel walls. (c) Schematic of the proposed cell sorting system using an analog electronic fluorescence detection method

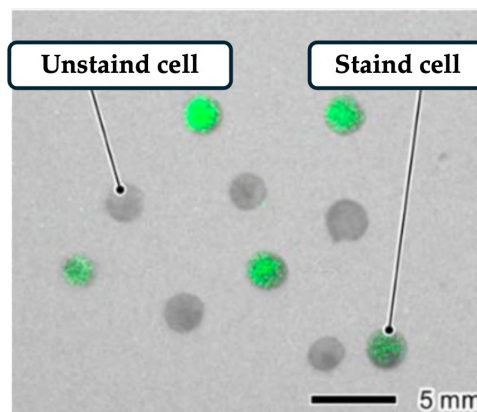


Figure 3 A snapshot of the stained and unstained cells

2.4 Analog electronic fluorescence detection

The optical detection circuit was constructed on a breadboard and comprised resistors, a CdS cell (photosensor), and transistors (Figure 5a). The resistance of the CdS cell changes with the intensity of the incident light, thereby converting optical signals into electrical signals. The transistors are active components that control and amplify the current. They were configured in a Darlington connection, where multiple transistors are connected in series to achieve a high current gain. This configuration enables the detection of weak fluorescence signals by producing

a large output current even with a low input signal (Figure 5b). The symbols used in Figure 5b are listed in Table 1. We detected fluorescence by irradiating the stained and unstained cells with an LED light source equipped with an excitation filter (469 ± 17.5 nm). The emitted fluorescence passed through a dichroic mirror, which reflected and transmitted light in the 452–490 and 505–800 nm ranges. It was then passed through an emission filter (525 ± 19.5 nm) before reaching the CdS cell.

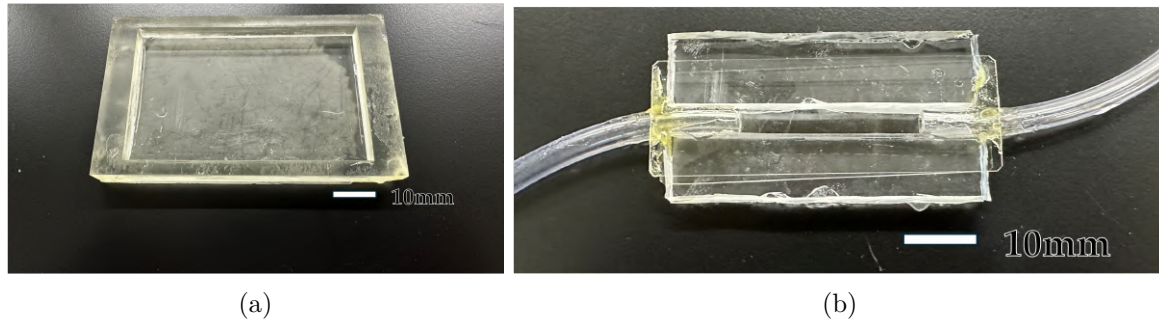


Figure 4 Photographs of (a) the mold and (b) the millifluidic device

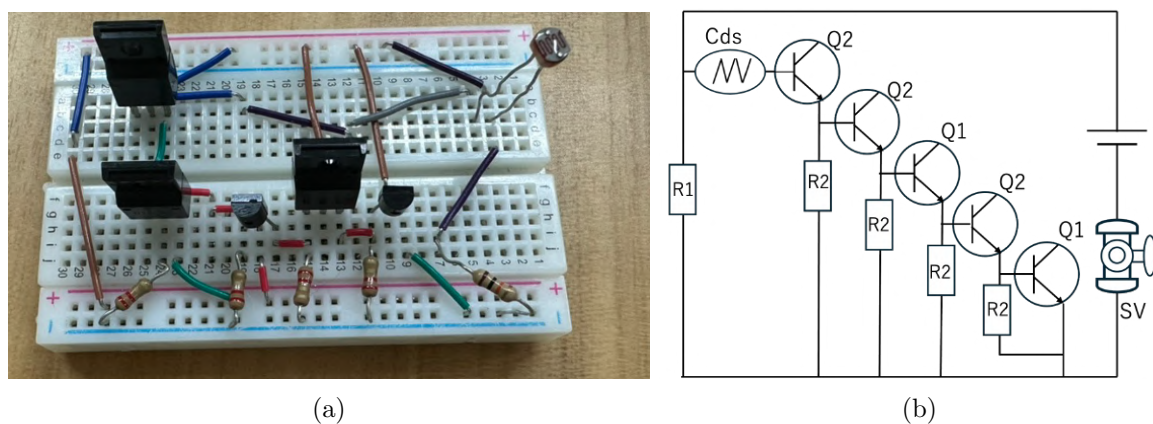


Figure 5 (a) Photograph of the optical detection circuit and (b) corresponding circuit diagram

Table 1 Description of the circuit diagram symbols used

Symbol	Component
R1	Resistor (10 k Ω)
R2	Resistor (2 Ω)
CdS	CdS cell
Q1	NPN transistor
Q2	Darlington transistor
SV	SV

2.5 Experiments

First, we examined the CdS cell response in a static setup, in which the cells were placed on a glass plate, 1 mm thick, to evaluate whether the developed optical detection circuit could distinguish between the stained and unstained cells. It was positioned above the CdS cell, and the current flowing to the solenoid valve was measured under irradiation with excitation wavelength light while examining three sample types: none, a single unstained cell, and a single stained cell placed on the glass plate (Figure 6a).

Next, we investigated whether the circuit could distinguish stained and unstained cells flowing through the millifluidic channel (Figure 6b). Five stained cells were introduced into the fabricated millifluidic device using a syringe pump (flow rate: 50 mL/min) at regular intervals, and alterations in current were measured as the cells passed through the detection area. Then, we evaluated whether the changes in current observed during the passage of stained cells are sufficient to control the solenoid valve.

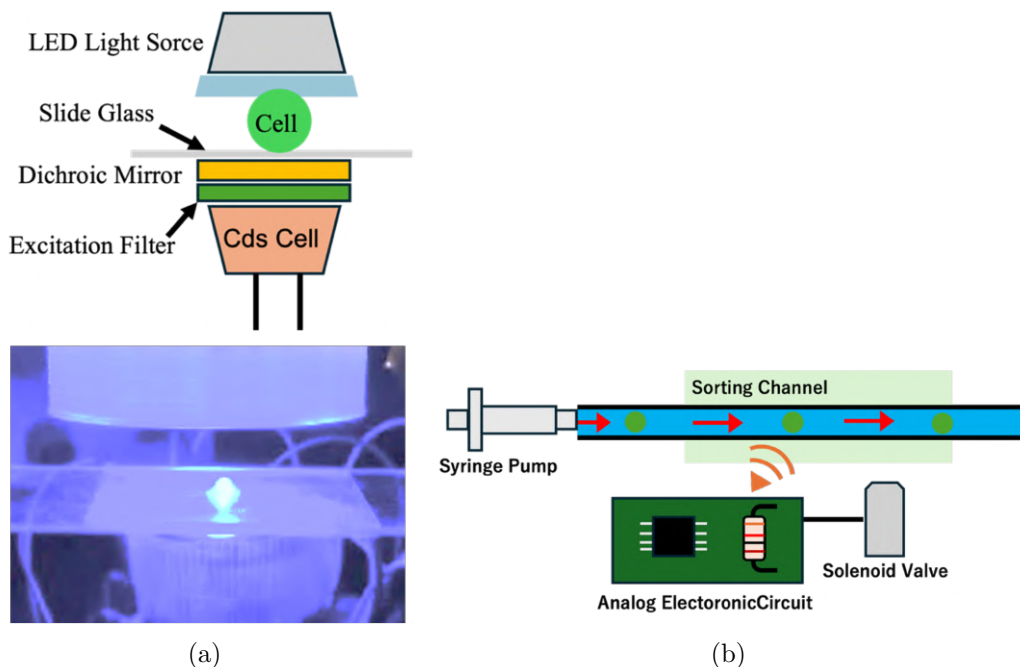


Figure 6 (a) Schematic and photograph of cell fluorescence detection in the static setup. (b) Schematic of fluorescence detection emitted by cells flowing through the millifluidic device

3. Results and Discussion

When only a glass plate was placed above the CdS cell and excitation light was applied, the measured current ranged from ~ 1 to 5 mA. However, when placed on the glass plate, the current increased to 15–20 mA for an unstained cell and to 62–66 mA for a stained cell. These results indicate that the fluorescence emitted by stationary cells can be detected as the current increases (Figure 7a).

The temporal changes in the current when the stained cells flowed through the millifluidic device are shown in Figure 7b. Sharp current spikes were observed when each of the five stained cells passed through the detection area. This finding indicates that the developed electronic circuit can detect cells flowing through the channel at a rate of ~ 2.85 cells/s without any delay. This observation confirms that the system can be applied to continuous cell detection and can sort cells at a rate of 0.35 s/cell, which is an order of magnitude faster than the previously reported rate of 3 s/cell, thereby representing a marked improvement in real-time performance. However, the use of flowing cells reduced the peak current values by ~ 5 mA compared to when the stained cells were placed on a glass plate. The threshold current of 60 mA required to open the solenoid valve was exceeded in only three of the five events. We identified two possible causes for the reduction in the peak current with the use of flowing cells. The first is the attenuation of the fluorescence signal by the buffer, in which the flowing cells were suspended and the stationary cells were placed in air. The second is the flow speed of the cells. A comparison of the peak current values and the corresponding cell flow speeds revealed that when the flow speed exceeded ~ 30 mm/s, the current did not reach the threshold required to activate the solenoid valve (Fig. 7d). These findings indicate that improving both the sensitivity of the optical detection circuit and controlling the cell flow speed are essential considerations for future work.

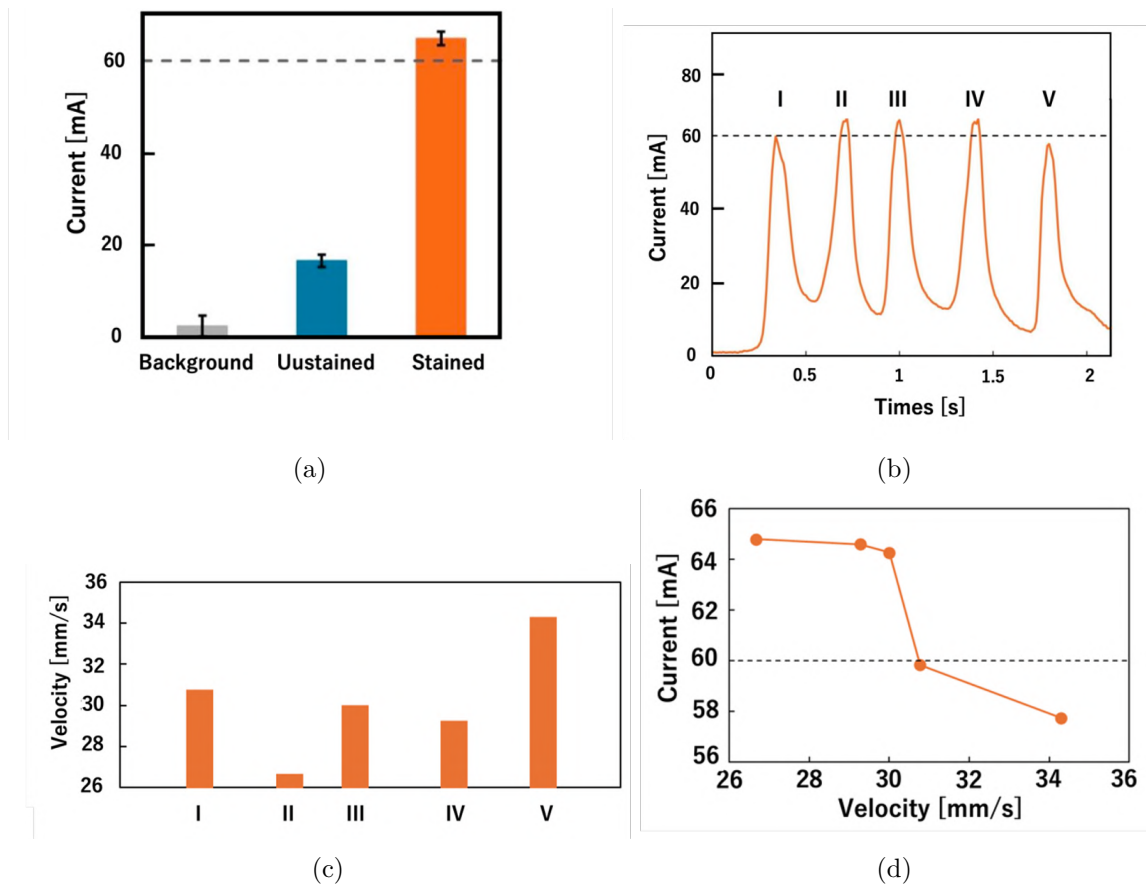


Figure 7 (a) Current values observed under static conditions. (b) Temporal change in the current when stained cells flowed through the millifluidic device. The dashed lines indicate the threshold current required to open the valve. (c) Flow speed of the cells at the times at which the current peaks are observed (Figure 8b). The Roman numerals correspond to the peak numbers labelled in Figure 8b. (d) Relationship between the observed peak current values and the corresponding cell flow speeds. The dashed line indicates the threshold current required to open the valve

4. Conclusions

In this study, the cell detection rate was successfully increased from 1.6 to 2.85 cells/s by replacing the conventional image processing-based detection method with an analog electronic fluorescence-based detection approach. However, the electronic circuit's fluorescence detection speed was not fully optimized, with considerable room for further improvement. The integration of this detection system into the sorting system developed in our previous study is yet to be accomplished. In future work, we aim to achieve high-speed sorting of large cells by advancing the electronic circuit, such as replacing the photosensor with a faster-response alternative, and post-implementation validation of its performance into the sorting system.

Author Contributions

1, Shinnosuke Dowaki: Conceptualized and designed the study, developed the methodology, validated the approach, conducted the investigation, prepared the original draft, and contributed to visualization. 2, Meito Fukada: Contributed to conceptualization and methodology, assisted in investigation, and contributed to visualization. 3, Taiji Okano: Originated the core research idea, made a major contribution to research planning, contributed to conceptualization and methodology, validated the approach, supervised the project, administered the project, and contributed to review and editing of the manuscript. 4, Yosuke Tanaka: Supervised the research, contributed to conceptualization, provided critical review and editing of the manuscript, and

served as the corresponding author.

Conflict of Interest

The authors declare no conflicts of interest.

References

- Azwani, W., Cahya, D. A., Gazali, A. D., Karima, A. P., Oktavya, G., Istiqomah, R. N., Bustami, A., Rizqy, F. A., Katili, P. A., Purnama, U., & Djer, M. M. (2025). Biomaterial characterization of decellularized human amniotic membrane seeded with fetal human cardiac fibroblasts for cardiac tissue engineering. *International Journal of Technology*, *16*(5), 1651–1664. <https://doi.org/10.14716/ijtech.v16i5.7808>
- Capek, D., Safroshkin, M., Morales-Navarrete, H., Toulany, N., Arutyunov, G., Kurzbach, A., Bihler, J., Hagauer, J., Kick, S., Jones, F., Jordan, B., & Muller, P. (2023). Embryonet: Using deep learning to link embryonic phenotypes to signaling pathways. *Nature Methods*, *20*, 815–823.
- Chen, D., Xu, L., Xuan, M., Chu, Q., & Xue, C. (2024). Unveiling the functional roles of patient-derived tumour organoids in assessing the tumour microenvironment and immunotherapy. *Clinical and Translational Medicine*, *14*(9), e1802. <https://doi.org/10.1002/ctm2.180>
- Cotta, G. C., Santos, R. C. T. D., Costa, G. M. C., & Lacerda, S. M. S. N. (2024). Reporter alleles in hipscs: Visual cues on development and disease. *International Journal of Molecular Sciences*, *25*(20), 11009. <https://doi.org/10.3390/ijms252011009>
- Dinca, M. A., Ardeleanu, M. N., Puchianu, D. C., & Predusca, G. (2025). Preliminary study on sensor-based detection of an adherent cell's pre-detachment moment in a mpwm microfluidic extraction system. *Sensors*, *25*(9), 2726. <https://doi.org/10.3390/s25092726>
- Diouf, A., Sadak, F., Gerena, E., Mannioui, A., Zizioli, D., Fassi, I., Boudaoud, M., Legnani, G., & Haliyo, S. (2024). Robotic sorting of zebrafish embryos. *Journal of Micro and Bio Robotics*, *20*, 3.
- Fukada, M., Saito, K., & Okano, T. (2021). Capsule vending machine-like device for cell release with equal intervals. *Proceedings of MicroTAS 2021*, 243–244.
- Gao, G., Shao, T., Li, T., & Wang, S. (2025). Harnessing optical forces with advanced nanophotonic structures: Principles and applications. *Discover Nano*, *20*, 76.
- Han, X., Zhou, Z., Fei, L., Sun, H., Wang, R., Chen, Y., Chen, H., Wang, J., Tang, H., Ge, W., Zhou, Y., Ye, F., Jiang, M., Wu, J., Xiao, Y., Jia, X., Zhang, T., Ma, X., Zhang, Q., . . . Guo, G. (2020). Construction of a human cell landscape at single-cell level. *Nature*, *581*, 303–309.
- Hanninen, A. (2024). Vibrational imaging of metabolites for improved microbial cell strains. *Journal of Biomedical Optics*, *29*(S2), S22711. <https://doi.org/10.1117/1.JBO.29.S2.S22711>
- He, J., Cai, S., Feng, H., Cai, B., Lin, L., Mai, Y., Fan, Y., Zhu, A., Huang, H., Shi, J., Li, D., Wei, Y., Li, Y., Zhao, Y., Pan, Y., Liu, H., Mo, X., He, X., Cao, S., . . . Chen, J. (2020). Single-cell analysis reveals bronchoalveolar epithelial dysfunction in covid-19 patients. *Protein and Cell*, *11*(9), 680–687. <https://doi.org/10.1007/s13238-020-00752-4>
- Isozaki, A., Mikami, H., Tezuka, H., Matsumura, H., Huang, K., Akamine, M., Hiramatsu, K., Iino, T., Ito, T., Karakawa, H., Kasai, Y., Li, Y., Nakagawa, Y., Ohnuki, S., Ota, T., Qian, Y., Sakuma, S., Sekiya, T., Shirasaki, Y., . . . Goda, K. (2020). Intelligent image-activated cell sorting 2.0. *Lab on a Chip*, *20*(13), 2263–2273. <https://doi.org/10.1039/d0lc00080a>
- Jones, R. A., Renshaw, M. J., Barry, D. J., & Smith, J. C. (2023). Automated staging of zebrafish embryos using machine learning. *Wellcome Open Research*, *7*, 275.

- Li, P., Li, X., Wang, F., Gao, M., Bai, Y., Zhang, Z., & Wei, Z. (2024). Enrichment of prime-edited mammalian cells with surrogate puror reporters. *International Journal of Biological Macromolecules*, *271*, 132474. <https://doi.org/10.12688/wellcomeopenres.18313.3>
- Liao, M., Liu, Y., Yuan, J., Wen, Y., Xu, G., Zhao, J., Cheng, L., Li, J., Wang, X., Wang, F., Liu, L., Amit, I., Zhang, S., & Zhang, Z. (2020). Single-cell landscape of bronchoalveolar immune cells in patients with covid-19. *Nature Medicine*, *26*, 842–844. <https://doi.org/10.1038/s41591-020-0901-9>
- Liu, J., Zhi, X., Fang, X., Li, W., Zhao, W., Liu, M., Lai, E., Fang, W., Wang, J., Zheng, Y., Zou, J., Fu, Q., & Cui, W. (2025). The application of microfluidic chips in primary urological cancer: Recent advances and future perspectives. *Smart Medicine*, *1*, 70010. <https://doi.org/10.1002/smmd.70010>
- Lu, N., Tay, H. M., Petchakup, C., He, L., Gong, L., Maw, K. K., Leong, S. Y., Lok, W. W., Ong, H. B., Guo, R., Li, K. H. H., & Hou, H. W. (2023). Label-free microfluidic cell sorting and detection for rapid blood analysis. *Lab on a Chip*, *23*, 1226–1257. <https://doi.org/10.1039/D2LC00904H>
- Lyu, Y., Yuan, X., Glidle, A., & Fu, Y. (2020). Automated raman based cell sorting with 3d microfluidics. *Lab on a Chip*, *20*(22), 4235–4245. <https://doi.org/10.1039/D0LC00679C>
- Naderi, A. M., Bu, H., Su, J., Huang, M. H., Vo, K., Trigo Torres, R. S., Chiao, J. C., Lee, J., Lau, M. P. H., Xu, X., & Cao, H. (2021). Deep learning-based framework for cardiac function assessment in embryonic zebrafish from heart beating videos. *Computers in Biology and Medicine*, *135*, 104565. <https://doi.org/10.1016/j.compbiomed.2021.104565>
- Napitupulu, M., Zai, F., Lestari, S. W., Witjaksono, L., Drakel, Z., Bhavnani, D., Yunihastuti, E., Pratama, G., Kodariah, R., & Kusmardi, K. (2025). Oxidative stress, dna fragmentation and caspase-3 regulation in hiv-1 positive men: A study of sperm preparation. *International Journal of Technology*, *16*(2), 639–651. <https://doi.org/10.14716/ijtech.v16i2.6420>
- Nguyen, T. D., Chooi, W. H., Jeon, H., Chen, J., Tan, J., Roxby, D. N., Lee, C. Y. P., Ng, S. Y., Chew, S. Y., & Han, J. (2024). Label-free and high-throughput removal of residual undifferentiated cells from ipsc-derived spinal cord progenitor cells. *Stem Cells Translational Medicine*, *13*(4), 387–398. <https://doi.org/10.1093/stcltm/szae002>
- Nie, X., Luo, Y., Shen, P., Han, C., Yu, D., & Xing, X. (2021). High-throughput dielectrophoretic cell sorting assisted by cell sliding on scalable electrode tracks made of conducting-pdms. *Sensors and Actuators B: Chemical*, *327*, 128873.
- Nitta, N., Iino, T., Isozaki, A., Yamagishi, M., Kitahama, Y., Sakuma, S., Suzuki, Y., Tezuka, H., Oikawa, M., Arai, F., Asai, T., Deng, D., Fukuzawa, H., Hase, M., Hasunuma, T., Hayakawa, T., Hiraki, K., Hiramatsu, K., Hoshino, Y., ... Goda, K. (2020). Raman image-activated cell sorting. *Nature Communications*, *11*(1), 3452. <https://doi.org/10.1038/s41467-020-17285-3>
- Nurhayati, R. W., Lubis, D. S. H., Pratama, G., Agustina, E., Khoiriyah, Z., Alawiyah, K., & Pawitan, J. A. (2021). The effects of static and dynamic culture systems on cell proliferation and conditioned media of umbilical cord-derived mesenchymal stem cells. *International Journal of Technology*, *12*(6). <https://doi.org/10.14716/ijtech.v12i6.5172>
- Park, S., Min, C. H., Choi, E., Choi, J. S., Park, K., Han, S., Choi, W., Jang, H. J., Cho, K. O., & Kim, M. (2025). Long-term tracking of neural and oligodendroglial development in large-scale human cerebral organoids by noninvasive volumetric imaging. *Scientific Reports*, *15*, 2536. <https://doi.org/10.1038/s41598-025-85455-8>
- Pragiwaksana, A., Irsyad, M., Nadhif, M., Muradi, A., Jasirwan, C. O. M., Juniantito, V., Syaiful, R. A., & Antarianto, R. D. (2024). Maintenance of hipsc-derived hepatocytes in a perfusion bioreactor integrated with stem cell hepatic intuitive apparatus. *International Journal of Technology*, *15*(5). <https://doi.org/10.14716/ijtech.v15i5.6088>
- Qiang, Y., Xu, M., Pochron, M. P., Jupelli, M., & Dao, M. (2024). A framework of computer vision-enhanced microfluidic approach for automated assessment of the transient sickling

- kinetics in sickle red blood cells. *Frontiers in Physics*, *12*, 1331047. <https://doi.org/10.3389/fphy.2024.1331047>
- Raffaele, I., Cipriano, G. L., Anchesi, I., Oddo, S., & Silvestro, S. (2025). Crispr/cas9 and ipsc-based therapeutic approaches in alzheimer's disease. *Antioxidants*, *14*(7), 781.
- Saito, K., Ota, Y., Turlousse, D. M., Matsukura, S., Fujitani, H., Morita, M., Tsuneda, S., & Noda, N. (2021). Microdroplet-based system for culturing of environmental microorganisms using fnap-sort. *Scientific Reports*, *11*(1), 9506. <https://doi.org/10.1038/s41598-021-88971-6>
- Shen, M. J., Olsthoorn, R. C. L., Zeng, Y., Bakkum, T., Kros, A., & Boyle, A. L. (2021). Magnetic-activated cell sorting using coiled-coil peptides: An alternative strategy for isolating cells with high efficiency and specificity. *ACS Applied Materials and Interfaces*, *13*(10), 11621–11630. <https://doi.org/10.1021/acsami.0c22185>
- Sibuea, C. V., Pawitan, J., Antarianto, R., Jasirwan, C. O. M., Sianipar, I. R., Luviah, E., Nurhayati, R. W., Mubarak, W., Fahdia, N., & Mazfufah, M. (2020). 3d co-culture of hepatocyte, a hepatic stellate cell line, and stem cells for developing a bioartificial liver prototype. *International Journal of Technology*, *11*(5), 951–962. <https://doi.org/10.14716/ijtech.v11i5.4317>
- Sivaramakrishnan, M., Kothandan, R., Govindarajan, D. K., Meganathan, Y., & Kandaswamy, K. (2020). Active microfluidic systems for cell sorting and separation. *Current Opinion in Biomedical Engineering*, *13*, 60–68. <https://doi.org/10.1016/j.cobme.2019.09.014>
- Vo, Q. D., Nakamura, K., Saito, Y., Iida, T., Yoshida, M., Amioka, N., Akagi, S., Miyoshi, T., & Yuasa, S. (2024). Ipsc-derived biological pacemaker—from bench to bedside. *Cells*, *13*(24), 2045. <https://doi.org/10.3390/cells13242045>
- Williams, M. G., Faber, Z. J., & Kelley, T. J. (2025). Comparison of artificial intelligence image processing with manual leucocyte differential to score immune cell infiltration in a mouse infection model of cystic fibrosis. *Journal of Pathology Informatics*, *17*, 100438. <https://doi.org/10.1016/j.jpi.2025.100438>
- Yousafzai, M. S., & Hammer, J. A. (2023). Using biosensors to study organoids, spheroids and organs-on-a-chip: A mechanobiology perspective. *Biosensors*, *13*(10), 905. <https://doi.org/10.3390/bios13100905>
- Zhang, J., Lin, H., Xu, J., Zhang, M., Ge, X., Zhang, C., Huang, W. E., & Cheng, J. X. (2024). High-throughput single-cell sorting by stimulated raman-activated cell ejection. *Science Advances*, *10*(50), adn6373. <https://doi.org/10.1126/sciadv.adn6373>